Reaction dynamics and the cage effect in microclusters of Br2Arn

ARTICLE *in* THE JOURNAL OF PHYSICAL CHEMISTRY · DECEMBER 1984

Impact Factor: 2.78 · DOI: 10.1021/j150670a041

2 AUTHORS, INCLUDING:

François G. Amar
University of Maine
46 PUBLICATIONS **937** CITATIONS

model to the trajectory data for $N(\tau)$ is compared with those of the two-state model and the $k_{MIC}(0)$-based curve in Figures 1 and 3. The smallness of the k_4 and k_5 values is responsible for the long-time tail in these plots.

When a model which is the three-state analogue of eq 17 is considered, one finds

$$1/k^0 = 1/k_{MIC}(0) + 1/k_3 \qquad k^\infty = 0 \tag{23}$$

instead of eq 22.

The three-state model in eq 10 and 18 could also be applied to the lifetime studies of an ensemble that was initially microcanonical rather than being produced by chemical activation. One could also test it to see whether the k_i's so obtained in a numerical fit to the trajectory data agree with those obtained above from a fit to the chemical activation study. However, an accurate lifetime distribution curve for the former was not given in ref 16.

5. Discussion and Summary

We have seen in ref 15 that a highly nonexponential lifetime distribution in a quasiclassical simulation of HCC unimolecular decomposition gave, nevertheless, chemical activation rate constants at low and high pressure which agreed with (k^0) or were not too different from (k^∞, factor of 4) the value of $k_{MIC}(0)$, the microcanonical rate constant at $\tau = 0$. Two- and three-state statistical models are described in the present paper, for which a slow energy transfer occurs between regions of phase space. They have a highly nonexponential lifetime distribution for both the microcanonical and chemical activation ensembles but, nevertheless, give a chemical activation rate constant in the low-pressure regime which agress analytically with the microcanonical $\tau = 0$ value. The three-state model was used to fit accurately the temporal behavior, including the long-time tail.[15] The model may also apply to other forms of excitation, such as high CH overtome excitation after a time interval for quantum-mechanical "dephasing" of the initial excitation.

Although such kinetic models may have a correct physical basis for some systems, in other cases it may be necessary to formulate a model which allows nonstatistical transitions in the phase space that are not simply described by kinetic schemes. This situation could arise when the intramolecular motion is so highly correlated that a trajectory undergoes infrequent (and hence nonstatistical) transitions between different types of motion which may themselves be nearly quasiperiodic or chaotic.[20]

The individual trajectories in ref 15 were not studied in sufficient detail to see whether one can identify three regions in phase space (if they indeed exist), for example, in terms of the various excitations of the coordinates mentioned earlier. In such a study one could use the spectral trajectory method,[21] applied to each of the relevant coordinates, to determine from the spectral intensities in the neighborhood of various frequencies the temporal behavior for occupation of the various parts of phase space.

Some caution is needed in the use of classical trajectory studies. The long-time tail in Figures 1 and 3 was due to "nearly trapped" trajectories. Quantum mechanically the system could also escape from such a trapping by tunneling to other parts of phase space. Again, another quantum-mechanical effect, one which could occur particularly at short rather than at long times, is a dephasing of a time evolving wave packet. The relation between the quantum-mechanical treatment and a kinetic model has been discussed in ref 22 for radiationless transitions.

We have not commented on the relation between $k_{MIC}(0)$ and the RRKM-calculated value of k appearing in eq 1, since this has been done in ref 19. The two values agree, within the error of the harmonic count in the calculation of k_{RRKM} in that reference. (A more accurate phase space count could be used to see the precise relation.) This result is not unexpected, since there was no recrossing[23] of the transition state in those trajectories. The microcanonical distribution of lifetimes in ref 16 was highly non-RRKM, a result consistent with the kinetic models used here and consistent with an equality of $k_{MIC}(0)$ and k_{RRKM}.

Acknowledgment. This research is supported by the National Science Foundation. The collaborative research presented here was initiated at the NATO workshop on "Primary Photophysical Processes" held at Herrsching, FRG, in 1983.

(20) Wolf, R. J.; Hase, W. L. *J. Chem. Phys.* **1980**, *73*, 3779. Cf.: Noid, D. W.; Koszykowski, M. L.; Marcus, R. A. *Annu. Rev. Phys. Chem.* **1981**, *32*, 267 for review on quasi-periodic and chaotic motion.

(21) Noid, D. W.; Koszykowski, M. L.; Marcus, R. A. *J. Chem. Phys.* **1977**, *67*, 404. Koszykowski, M. L.; Noid, D. W.; Marcus, R. A. *J. Phys. Chem.* **1982**, *86*, 2113. Wardlaw, D. W.; Noid, D. W.; Marcus, R. A. *Ibid.* **1984**, *88*, 536. Cf. an application of Noid's method (Noid, D. W. Ph.D. Thesis, University of Illinois, Urbana, IL, 1976) in: McDonald, J. D.; Marcus, R. A. *J. Chem. Phys.* **1976**, *65*, 2180.

(22) Lahmani, F.; Tramer, A.; Tric, C. *J. Chem. Phys.* **1974**, *60*, 4431.

(23) A review of this point is given in: Truhlar, D. G.; Garrett, B. C. *Acc. Chem. Res.* **1980**, *13*, 440. Hase, W. L. *Acc. Chem. Res.* **1983**, *16*, 258.

Reaction Dynamics and the Cage Effect in Microclusters of Br_2Ar_n

François G. Amar† and Bruce J. Berne*

Department of Chemistry, Columbia University, New York, New York 10027 *(Received: August 6, 1984)*

We present the results of a molecular dynamics trajectory study of the photodissociation/recombination reaction of Br_2 in argon clusters. Initial conditions of the clusters correspond to the cold, collision-free regime obtainable in a supersonic molecular beam. We compare our results to gas- and liquid-phase studies.

Introduction

One of the important problems in chemical physics is the microscopic description of solvent effects on chemical reactions. Isomerization reactions have been studied extensively with a view to sorting out the respective roles of intramolecular energy-transfer processes and solvent–solute interactions.[1] The photodissociation of I_2 in various solvents has received a great deal of attention, both experimental[2-5] and theoretical[5-11] in recent years. Studies of this

† Present address: Department of Chemistry, University of Maine at Orono, Orono, ME 04469.

(1) Berne, B. J.; De Leon, N.; Rosenberg, R. O. *J. Phys. Chem.* **1982**, *86*, 2166.

(2) Chuang, T. J.; Hoffman, G. W.; Eisenthal, K. B. *Chem. Phys. Lett.* **1974**, *25*, 201.

(3) Langhoff, C. A.; Moore, B.; Nugent, W. In "Picosecond Phenomena"; Hochstrasser, R., Ed.; Springer-Verlag: West Berlin, 1980; Vol. II, p 249.

(4) Kelley, D. F.; Rentzepis, P. M. *Chem. Phys. Lett.* **1982**, *85*, 85.

0022-3654/84/2088-6720$01.50/0

system have yielded much information about the so-called "cage effect".

It would be natural to assume that the probability of recombination of a diatomic molecule decreases with excitation energy. The present study demonstrates an important caveat. Recombination is in fact controllled by impulsive collisions with the solvent cage, and it is the ratio of kinetic to potential energy which determines the geminate recombination probability. A simple model describing this effect will be outlined below.

The picosecond laser experiments of Eisenthal and co-workers[2] showed that for I_2 in CCl_4 following an excitation pulse at 530 nm, the change in transmission decayed with a lifetime of 100 ps. This decay was ascribed to the recombination of I_2 following caging by solvent molecules: absorbers which had been removed by the excitation pulse return gradually to the ground state to be detected by the time-delayed probe pulse. Thus, the time scale for geminate recombination of I_2 in CCl_4 was thought to be about 100 ps. Nesbitt and Hynes' simulation of the relaxation of I_2 initially excited near the dissociation limit of the ground state showed that it takes about 1000 ps for the molecule to decay to vibrational levels where there is significant Franck–Condon overlap with the excited state in a structureless CCl_4 solvent (V–T transfer). When internal CCl_4 vibrations were included, however, a decay time of the order of 100 ps was found (V–V transfer).[7]

The picture that emerges is the following: excitation to some excited state, followed by relatively fast (10–20 ps) relaxation in the upper state, curve hopping to the ground state (highly vibrationally excited), and finally slower relaxation down the ground-state vibrational ladder to the range of vibrational quantum states where the probe laser can excite the molecule again. This picture is substantially confirmed by the molecular dynamics simulations of Wilson and co-workers,[5] in which I_2 photodissociation and recombination reactions were studied in a structureless solvent (xenon). Kelley and Rentzepis recently performed an experiment similar to Eisenthal's but in xenon liquid and dense xenon gas: they report a 40-ps decay of the transmission—in complete contradiction to the picture that has emerged from the simulations.[4] It should be noted that these experiments involved excitation to the B and repulsive $^1\Pi_{1u}$ states of I_2, and the subsequent dynamics can be very complicated. Flynn and co-workers, among others, have postulated that matrix-isolated halogen molecules that have been excited to the B and $^1\Pi_{1u}$ states have very complicated relaxation dynamics including trapping in lower excited states.[12] The simulation work has, for simplicity, ignored many of these complicating factors, including the possibility of absorption by these excited states in the wavelength region of interest.

Other workers have looked at different aspects of this problem: Troe et al.[13] measured geminate recombination rates in dense gases, and recently Sceats and co-workers[11] have applied simulation techniques in the grand canonical ensemble to this problem. Adelman and co-workers have applied the MTGLE version of the Zwanzig Mori formalism to the problem of cage formation and disruption in liquids.[10] It is our belief that a study of similar reactions in a molecular cluster (as can be prepared in molecular beams) will contribute significantly to our understanding of solvation effects in such bond-breaking reactions. This paper presents results of a simulation of such a reaction by means of molecular dynamics (MD) techniques.

TABLE I: Potential Function Parameters for Br_2

state	D_e, K	r_e, Å	α, Å^{-1}	E_0, K	ref
$X^1\Sigma_g^+$	23100	2.28	1.94	23100	19
$B^3\Pi_{0u}^+$	5521	2.68	2.05	221	18
$A^3\Pi_{1u}$	3093	2.695	2.567	3093	18

The reaction that we are considering is the unimolecular decay of an activated cluster molecule:

$$Br_2Ar_n \rightarrow Br_iAr_m + Br_{2-i}Ar_l + (n - m - l)Ar \qquad (i = 0, 1, 2)$$

The Br_2Ar_n is initially cold and is then excited by a "laser" to some upper vibronic state where it may undergo some or all of the following processes: (1) dissociation of Br_2 with or without escape of Br radical from the cluster; (2) energy transfer of excess electronic and vibrational energy of Br_2 to the van der Waals modes of the cluster resulting in heating of the cluster and loss of Ar atoms by evaporation; (3) electronic curve crossing back to ground state resulting in "geminate" recombination of the Br radicals; (4) vibrational energy transfer from Br_2 to the van der Waals modes resulting in continued heating of the cluster. Which processes occur (and to what degree) depends on several factors. As in the liquid-state reaction, initial excitation energy is important as is the solvent temperature. Unlike the liquid case, however, in the cluster the number of solvent atoms around the Br_2 can be varied. Two very important effects can be studied in this way. First, the effect of adding more solvent atoms on the Br_2 reaction dynamics can be studied, allowing the determination of the number of solvent shells necessary to cage the Br_2 effectively. Second, the relaxation behavior of those molecules that do recombine may vary dramatically with cluster size, temperature, and initial excitation energy. In contrast to the condensed phase, the only way to dissipate the energy of the cluster is by evaporation of atoms; there is no extended heat bath in which to dissipate this energy as it is released by the Br_2. Consequences of this fact will be discussed in a later section.

Supersonic beam technology combined with laser-induced fluorescence (LIF) and multiphoton ionization (MPI) techniques make it possible to study the structure and reaction dynamics of molecules as a function of cluster size ranging from the isolated molecule to partially solvated molecules to molecules embedded in clusters so large as to be "bulklike". The transition from isolated-molecule to solvated-molecule behavior has been extensively studied in the past 10 years.[14-16] Increased knowledge of the properties of clusters should lead to significant advances in our understanding of the condensed phase and should have applications in other areas of energy-transfer processes.

The outline of this paper is as follows: In section II we describe the reaction system and the computational methods used. Section III describes the results of our initial state preparation and expectations based on a simple hard-sphere collision model. Excitation and recombination dynamics are discussed in section IV. Section V is a presentation of our findings concerning the vibrational relaxation of recombined bromine molecules in clusters, and we summarize our results in section VI.

II. Methodology

The main purpose of this paper is to investigate the dynamics of the dissociation and recombination of Br_2 in argon clusters of varying size and internal energy. To do this we integrate Hamilton's equations of motion:

$$\dot{q}_i = \partial H/\partial p_i; \qquad \dot{p}_i = -\partial H/\partial q_i \qquad (i = 1, 3N) \qquad (1)$$

(5) Bado, P.; Berens, P. H.; Wilson, K. R. *Proc. Soc. Photo-Optic. Instrum. Eng.* **1982**, 322 and references contained therein.
(6) Bado, P.; Berens, P. H.; Bergsma, J. P.; Wilson, S. B.; Wilson, K. R.; Heller, E. J. In "Picosecond Phenomena"; Eisenthal, K., Hochstrasser, R., Kaiser, W., Laubereau, A., Eds.; Springer-Verlag: West Berlin, 1982.
(7) Nesbitt, D. J.; Hynes, J. T. *J. Chem. Phys.* **1982**, *77*, 2130.
(8) Murrell, J. N.; Stace, A. J.; Dammel, R. *J. Chem. Soc., Faraday Trans 1* **1978**, *74*, 1532.
(9) Bunker, D. L.; Jacobson, B. S. *J. Am. Chem. Soc.* **1972**, *94*, 1843.
(10) Brooks, C. L.; Adelman, S. A. *J. Chem. Phys.* **1982**, *77*, 484.
(11) Lipkus, A. H.; Buff, F. P.; Sceats, M. *J. Chem. Phys.* **1983**, *79*, 4830.
(12) Beeken, P.; Hansen, E. A.; Flynn, G. W.; *J. Chem. Phys.* **1981**, *78*, 5892. Beeken, P.; Mandich, M.; Flynn, G. W. *J. Chem. Phys.* **1982**, *76*, 5995. Mandich, M.; Beeken, P.; Flynn, G. W. *J. Chem. Phys.* **1983**, *77*, 702.
(13) Luther, K.; Troe, J. *Chem. Phys. Lett.* **1974**, *24*, 85.
(14) Levy, D. In "Quantum Dynamics of Molecules"; Woolley, R. G., Ed.; Phenum Press: New York, 1980; NATO ASI Ser. B, Vol. 57 and references contained therein.
(15) Amirav, A.; Even, U.; Jortner, J. *Chem. Phys. Lett.* **1980**; *72*, 16.
(16) Gough, T. E.; Knight, D. G.; Scoles, G. *Chem. Phys. Lett.* **1983**, *97*, 155.
(17) LeRoy, R.; Macdonald, R.; Burns, G. *J. Mol. Spectrosc.* **1979**, *51*, 428, *J. Chem. Phys.* **1976**, *65*, 1485.

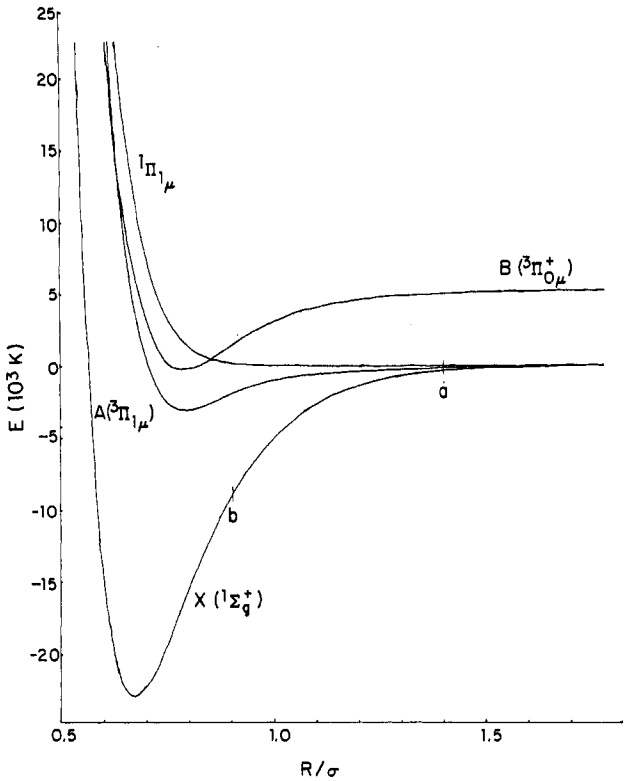

Figure 1. Potential energy curves for four electronic states of Br_2. The σ alues for the Ar–Ar and Br–Ar interactions are as indicated. Also indicated are (a) the recombination distance of 1.4σ (see section IV) and (b) the Br_2 bond distance at which collision with the cap atoms occurs in the 10 K Br_2Ar_{20} cluster.

where N is the total number of atoms in the system and H is given by

$$H = \sum_{i=1}^{3N} p_i^2/2m_i + V(q) \tag{2}$$

We take V to be a sum of pairwise interactions: The X, B, and A states of bromine are represented in this calculation by Morse functions;[18,19]

$$V(r) = D\{1 - \exp[-\alpha(r - r_e)]\}^2 - E_0 \tag{3}$$

where E_0 shifts the curve so that the zero of energy is the dissociation limit of the X state. Parameters are given in Table I. The repulsive $^1\Pi_{1u}$ state is represented by the function[17]

$$V(r) = V_0 \exp[-\alpha(r - r_0) - \beta(r - r_0)^2] \tag{4}$$

where $V_0 = 11012.95$ K, $r_0 = 2.3$ Å, $\alpha = 4.637$ Å^{-1}, $\beta = 0.879$ Å^{-2}. The Ar–Ar interaction[20] is represented by a Lennard-Jones potential ($\epsilon = 119.8$ K, $\sigma = 3.405$ Å) as is the Br–Ar interaction[21] ($\epsilon' = 143$ K, $\sigma' = 3.51$ Å). (See Figure 1.)

Let us note the following about energy scales and units. Our basic unit of energy is the Ar–Ar well depth, ϵ; in this unit the dissociation energy of the Br_2 ground state is $D_e = 192\ \epsilon$. The total energy of the Franck–Condon transition from the ground state to the $^1\Pi_{1u}$ state repulsive wall is about $1.5D_e$ ($288\ \epsilon$). The energy required to remove one argon atom from the cluster is on the order of 4–5 ϵ. Finally, it is useful to remark that the Br–Ar potential is similar to the Ar–Ar potential; this means that a Br atom looks very much like an argon atom to another argon.

In order to carry out molecular dynamics calculations on clusters we need a set of initial positions and momenta. We choose such sets via a three-step procedure. First we perform a Metropolis Monte Carlo[22] calculation on each cluster size to be considered. This allows us to sample configuration space very efficiently in order to find stable (though not necessarily the most stable) geometric isomers of the Br_2Ar_N cluster. The structure of the cluster plays an important role in the subsequent dynamics; we take up this question in section III. Second, we sample random momenta for each particle from a Gaussian distribution.[22] The phase point generated in this way is used to start a molecular dynamics (MD) trajectory[22] which is in turn adjusted so that the time average of its kinetic energy will yield a predetermined temperature:

$$\sum_i \langle p_i^2/2m_i \rangle = (3N - 3)kT/2 \tag{5}$$

Finally, phase points to be used as initial conditions for MD trajectories with simulated photoexcitation are chosen, well spaced in time, from a single trajectory for which the temperature defined by eq 5 has converged. At a temperature of 10 K, sets of up to about 100 initial conditions were chosen at intervals of about 3 ps. Since 10 K clusters are in a microcrystalline state, the configurations of these initial clusters appear rather similar. The characteristic time for vibration of the van der Waals modes of the cluster is on the order of 3 ps, so we expect that this sampling procedure will lead to uncorrelated initial phases for the cluster vibrations. This is confirmed by the lack of systematic correlation in the excitation dynamics of successive trajectories.

The procedure just described amounts to equilibrating a Br_2Ar_N cluster at a given total energy which corresponds to the most probable energy of a distribution of clusters at temperature T. Excitation trajectories are started by simulating a Franck–Condon transition to some excited state and then integrating the equations of motion. A classical Franck–Condon transition for Br_2 is realized in the simulation by changing instantaneously the interaction potential for the Br_2 molecule, but keeping the Br–Br interatomic distance and relative momentum invariant. We also performed some hypothetical excitations to the continuum of the X state: the energy of the excitation was chosen tc correspond to the energy of the X $\rightarrow$ $^1\Pi_{1u}$ transition, but the energy was put into the molecule by rescaling the relative momenta of the two bromine atoms such that the desired energy is achieved and the center of mass motion of the diatomic remains unaffected.

Let us note here that when bromine is highly excited, the system we are integrating is a very "stiff" system because of the large forces exerted on the Br_2 molecule at its inner turning point. A much smaller time step for the integrator is required than would be necessary for an isolated argon cluster. Using a time step of about 3×10^{-15} s, energy conservation was maintained at 1 part in 10^6 over a run of 20 000 steps (15 ps). For the largest clusters studied (70 argon atoms), the time step was increased by a factor of 3 resulting in the loss of one decimal digit of accuracy. All integrations were performed by using a fourth-order Adams–Moulton predictor-corrector method preceded by a Runge–Kutta integration for four time steps to initialize the integrator. It is important to note that the dynamics of the clusters using this accurate algorithm differed considerably from the dynamics using the Verlet algorithm. This arises from the need to follow many periods of vibration and thus raises questions about recent simulations of photochemistry in bulk systems using the less accurate Verlet algorithm.

III. Cold Cluster Geometry

In order to obtain initial conditions corresponding to cold clusters, we select a set of points from a spherical lattice, following

(18) The A and B states are fitted to data of ref 17 by: Bruskin, E. Ph.D. Thesis, Columbia University, New York, NY, 1984.
(19) Herman, M.; Berne, B. J. *J. Chem. Phys.* **1983**, *78*, 4103.
(20) Kaelberer, J. B.; Etters, R. D. *J. Chem. Phys.* **1977**, *66*, 3233.
(21) Freasier, B. C.; Jolly, D. C.; Hauer, N. D., Nordholm, S. *Chem. Phys.* **1979**, *38*, 293.

(22) For a discussion of Monte Carlo techniques see: Valleau, J. P.; Whittington, S. G. In "Statistical Mechanics, Part A; Equilibrium Techniques"; Berne, B. J., Ed.; Plenum Press: New York, 1977. For a discussion of Molecular Dynamics see: Kushick, J.; Berne, B. J. In "Statistical Mechanics, Part B: Time-Dependent Processes"; Berne, B. J., Ed.; Plenum Press: New York, 1977.

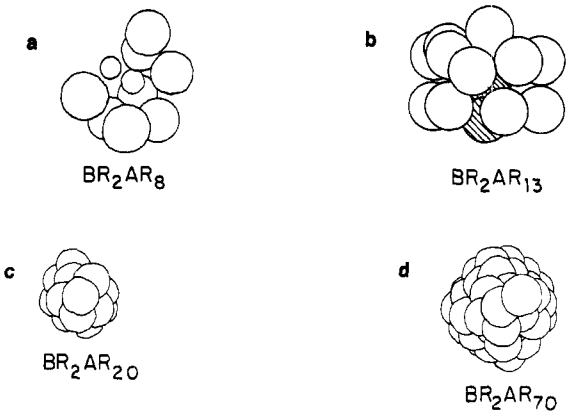

Figure 2. Equilibrium geometries of Br_2Ar_N clusters, N = 8, 13, 20, 70. Configurations from well-equilibrated Monte Carlo runs at 10 K. Note: radius of Br atoms drawn $^1/_2$ scale in Br_2Ar_8 cluster. For the Br_2Ar_8 cluster, the Br atoms are shaded. Also, the Br_2Ar_{20} and Br_2Ar_{70} pictures are rotated so that the Br_2 bond is oriented as in the Br_2Ar_8 case.

the procedure given by Abraham.[23] The lattice spacing is adjusted appropriately for argon and then two argons are removed from the center of the cluster and are replaced with a bromine molecule. Each particle is then moved in turn according to the Metropolis MC algorithm with different step sizes for Br and Ar, both adjusted to give acceptance ratios of about 0.5. The energy starts at the lattice value and then drops, with some fluctuations, to its equilibrium value. Figure 2 shows equilibrium configurations for four different clusters: Br_2Ar_8, Br_2Ar_{13}, Br_2Ar_{20}, and Br_2Ar_{70}. These four clusters show major qualitative differences in their structures and are typical of distinct size ranges. When the number of argons in a cluster is between 0 and 8, the Br_2 is said to be *uncapped*, between 9 and 16 it is said to be *half-capped*, and for Br_2Ar_{17} and larger clusters the structure is *doubly capped*.

Consider what happens when a laser excites the Br_2 molecule from its ground state to the repulsive wall of the $^1\Pi_{1u}$ state (i.e., a classical Franck–Condon excitation). In a classical description (which should be valid for Br_2 at this energy) the Br atoms begin to separate with velocity that increases until they reach the flat part of the potential, where they achieve a constant velocity. This is the case for an isolated molecule in a collision-free regime. In a cluster the situation is quite different. The Br atoms will suffer collisions with the argon solvent cage. The big question concerning recombination is this: how much energy will a Br atom lose when it collides with the cage? We shall consider this question for each size range separately beginning with the extreme cases of uncapped and double capped structures.

A. Uncapped Structures. The Br_2Ar_8 cluster shown in Figure 2a has all the argon atoms arranged around the "waist" of the bromine molecule, that is, roughly in the plane of symmetry of Br_2 and forming a chain of atoms around the axis of symmetry. Significantly, no argon atoms lie on either side of the bromine molecule along the lines of centers. Therefore, when Br_2 is excited, the only forces impeding the separation of the two radicals are the weak van der Waals attractions of the ring atoms which will provide a barrier of about 10 ϵ for the escape of Br atoms from the cluster. At very high ($1.5D_e$) excitation energies, therefore, Br atoms will leave the cluster with large velocities and correspondingly high kinetic energies. If the Br_2 is excited to lower energies (imagine, for example, excitation at different wavelengths into the continuum of the $A^3\Pi_{1u}$ state), the kinetic energy of the escaping Br atoms will decrease until some excitation threshold where the velocity is less than the escape velocity (determined by the attractive forces).

During this process, argon atoms may be lost as well. For the case in which the Br_2 is excited to the repulsive $^1\Pi_{1u}$ state, there will be only one "pass" in which the Br atoms may exchange energy with the argon shell before the bromines leave the cluster; this collision is likely to be a soft one, given the geometry of the cluster (large impact parameter, $b > \sigma'$ collision) so the velocity of an escaping argon will be quite low.

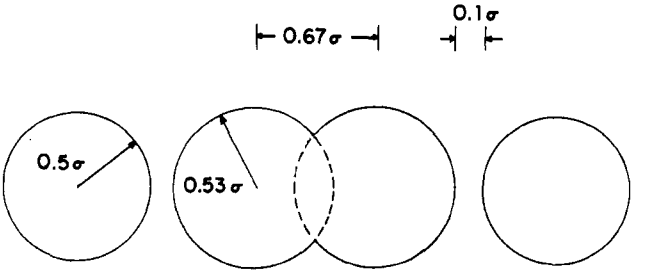

Figure 3. Relative positions of the Br_2 molecule and the two "cap" atoms are shown for a 10 K Br_2Ar_{20} cluster. The radii shown are from the Lennard-Jones σ values for the Ar–Ar and the Ar–Br interactions. If the Br_2 molecule begins to dissociate, the cap argon atoms will be "struck" when the Br_2 bond distance is approximately 0.9σ.

B. Doubly Capped Structures. These structures are far more interesting than the open ones discussed above, as the potential for a variety of dynamical effects is greater. Whether the molecule is excited by a Franck–Condon transition to the $^1\Pi_{1u}$, A, or B states or is hypothetically excited to the continuum of the X state, we may divide the dynamics into two parts: the initial violent collision with the solvent cage, and all the rest. The dynamics of the initial collision obviously depends in a detailed way on the geometry of the cluster. The initial geometry will thus play a major part in determining which processes (e.g., recombination, solvation, escape, evaporation of solvent atoms) will play a role and on what time scale they will occur.

Let us focus on the short-time behavior of the Br_2Ar_{20} cluster shown in Figure 2c. This cluster is a representative doubly capped structure. It consists of a bromine molecule with a single complete shell of argon atoms around it. Six argon atoms are arranged in a ring around the waist of the cluster and two additional rings of six atoms, rotated by 30° with respect to the center ring, are nestled above and below the waist. These 18 atoms form a kind of cylinder surrounding the Br_2; each end of the cylinder is then capped by an argon atom. At 10 K the fluctuations from this equilibrium configuration are rather small and the energy of the cluster is about -240 ϵ. The zero of energy is taken to be the separated atoms so we see that the Br_2 contributes -192 ϵ to the total energy and the van der Waals bonds contribute approximately -50 ϵ. Figure 3 shows a cross-sectional view of selected atoms from the Br_2Ar_{20} cluster in a plane through the axis of symmetry (the two bromine atoms and the two argon cap atoms are shown). The radii shown are the σ values for the Lennard-Jones potentials used in this calculation while the atoms are placed at their equilibrium positions.

The most important feature of Figure 3 is that is shows the distance between the Br atoms and the two collinear argon (cap) atoms. It is clear that the cap atoms are quite close to the Br atoms and that strong repulsion between the Br atoms and the cage will occur when $r^*_{Br-Br} \cong 0.95\sigma$. The consequences of this are quite dramatic and may best be appreciated by the case of continuum excitation of Br_2 to $1.5D_e$ in the X state. This excitation energy is the same as that of Franck–Condon transition to the $^1\Pi_{1u}$ state (see Figure 1) but with most of the energy in the Br–Br bond as kinetic instead of potential energy.

We can gain insight into the dynamics of the collision if we consider it to be a hard-sphere axial collision of Br with an Ar at the distance $r_{Ar-Br} = \sigma'$. Figure 3 also shows the r_{Br-Br} distance at which the r_{Ar-Br} distance criterion is met for the Br_2Ar_{20} configuration. Now, recall that for a hard-sphere collision, we need only specify the masses and the initial velocities of the two particles in order to determine the final velocities. In the case of bromine and argon where $m_{Br} = 2m_{Ar}$, $v_{Ar} = 0$, and $v_{Br} = [(E - V(r_{Br-Br}))/m_{Br}]^{1/2}$, we easily find that the final kinetic energy of the argon initially at rest is 8/9 of the kinetic energy of the Br before the collision (at the moment of impact). Thus, according

(23) Abraham, F. F. "Homogenous Nucleation Theory"; Academic Press: New York, 1974.

to this simple model, 8/9 of the kinetic energy of the Br atom is given up to the cap argon atom at the moment of impact. When the collision occurs in the X state, the initial kinetic energy is not simply the energy above the dissociation limit but also includes an additional contribution ($D_e - V(r^*_{Br-Br})$) due to the fact that the collision occurs when the Br_2 is still in the attractive region of its potential. For the geometry of Figure 3, this comes to an additional 84 ϵ. According to the hard-collision model, then, the bromine molecule will end up at lower energy than the dissociation limit, leading to immediate recombination.

The case described above is the extreme: if all of the excitation energy is kinetic energy, this model predicts that an excitation of about $5D_e$ would be required in order to observe Br atoms escaping. This estimate is made by solving the equation $E - V = 9(D_e - V)$ for $V = V(0.9\sigma)$. This result is obtained even with the neglect of the attractive forces due to the argon atoms (which would further raise the threshold of excitation necessary to observe dissociation). Several factors serve to soften this result: (1) Nonaxial collisions will be less effective in removing energy from the Br–Br bond coordinate; (2) more importantly, experimentally, it would be difficult if not impossible to excite a Br_2 molecule to the continuum of the X state. The experimentally feasible excitation schemes involve transitions to the A state, and to the B and $^1\Pi_{1u}$ states. The hard-sphere model says nothing about the dependence of dissociation on the total kinetic energy of the collision; rather it is the ratio $(D_e - V)/(E - V)$ that is important: the threshold value changes as the inverse of this ratio. The qualitative prediction for Br_2Ar_{20} excited to the A, B, and $^1\Pi_{1u}$ states, then, is that the recombination probability is largest for the B state, then the A, and finally lowest for the $^1\Pi_{1u}$ state, since the ratio $(D_e - V)/(E - V)$ is negative for the $^1\Pi_{1u}$ state.

Figure 2d shows the equilibrium geometry of a Br_2Ar_{70} cluster at 10 K. Note that is has the appearance of a distorted octahedral microcrystallite. Since this cluster is also doubly capped (we purposely prepared a rather symmetrical cluster), the initial caging step following excitation can be expected to mirror very closely that described for the Br_2Ar_{20} cluster. Very different dynamics may follow, however, as the Br_2 relaxes in the X state. This will be discussed below.

C. Half-Capped Structures. For clusters with between 9 and 16 argon atoms, the Br_2 molecule is capped only on one side. If the excitation of the bromine is achieved in such a way that the energy is given symmetrically to both atoms (as is assumed), then the kinetic energy arguments used in section IIIB may be applied to the Br that is capped, and the dissociation threshold (due to van der Waals attractions) arguments of section IIIA can be applied to the open Br. At low energy we expect no Br atoms to leave the cluster, and at higher energies we should see only one bromine atom leave the cluster. Only at very high energy will the capped bromine atom be able to retain enough kinetic energy to leave the cluster. Strong repulsion between the capped Br atoms and the cage will occur when $r^*_{Br-Br} \cong 0.9\sigma$.

IV. Excitation Dynamics and Recombination

In this section we first discuss the procedure for simulating the Br_2 excitation step. The Br_2 is initially vibrationally cold within a cold cluster—energy is equipartitioned among all the modes of the cluster and the center of mass of the entire cluster is fixed at the origin. The simplest way to excite the Br_2 is to shift it vertically to a new potential curve, keeping the bond coordinate and momentum fixed: a classical Franck–Condon transition. Alternatively, as described above, we may hypothetically excite to the continuum of the X state.

Consider now the second major set of assumptions about dynamics that we are forced to make in order to make progress. We are interested, ultimately, in the ratio of dissociating molecules to molecules that recombine. What is the mechanism of recombination? Clearly if we excite to the $^1\Pi_{1u}$ state we need to know how the Br_2 returns to the X state again. Presumably this occurs out in the tail of the potential where the curves are close in energy; in fact we cannot do a quantum-mechanical calculation to elucidate this mechanism, so we make the assumption that a Br_2 molecule whose bond distance reaches a specified value (in our case 1.4σ) automatically crosses to the lower state moving in the same direction with increased speed. This assumption is similar to the minimum time assumption made by Wilson and co-workers.[5] This does not imply recombination, since the Br atoms may continue to move apart on the flat part of the attractive curve. For excitation to the A state that situation is similar to that for the $^1\Pi_{1u}$ state, but for excitation to the B state, two curve-hopping steps are required, first from B to $^1\Pi_{1u}$, and then from $^1\Pi_{1u}$ to X.

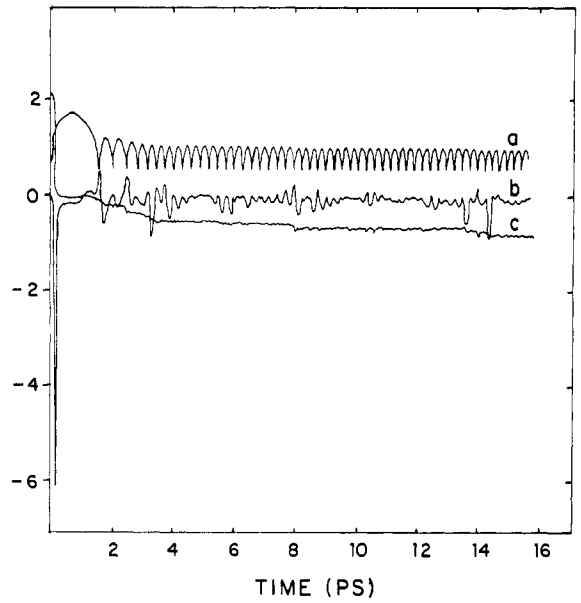

Figure 4. Excitation and recombination dynamics of 10 K Br_2Ar_{20} cluster excited to the repulsive $^1\Pi_{1u}$ state: (a) Br_2 bond distance in σ units vs. time (picoseconds); (b) force projection f_{bond} as defined in eq 6 in Verlet units.[22] (c) Br_2 bond energy in Verlet units (unit = 48 ϵ or bromine X state D_e = 4.017 units).

A. Br_2Ar_{20} Recombination Dynamics. We shall first consider the behavior of trajectories resulting from the classical Franck–Condon excitation of bromine embedded in a 20-argon cluster to the $^1\Pi_{1u}$ state, with crossover to the X state occurring at $r_{Br-Br} = 1.4\sigma$ as discussed above. Figure 4 shows the time dependence of several quantities of interest for a typical trajectory. Note that the value of r_{Br-Br} increases immediately following the excitation (at $t = 0$) as the Br atoms move apart along the repulsive curve. The bromine bond reaches maximum extension of about 2σ at 1 ps and then shortens to a cusplike minimum. The molecule has by this time collided with the cage, transferred to the X state, and reached the repulsive wall inner turning point. Also shown is the force projection:

$$f_{bond} = \sum_{Br}\sum_{Ar} \vec{F}_{Br-Ar} \cdot \hat{r}_{Br-Ar} \qquad (6)$$

This quantity is the component of the sum of the Br–Ar forces along the Br_2 bond stretch coordinate. It shows a sharp negative spike (width = 0.05 ps) at the time of the collision. Also shown is the Br_2 bond energy. The recombination step is completed in about 2 ps, and then the molecule relaxes within the cluster, heating up the van der Waals modes.

Let us now consider a second trajectory shown in Figure 5. This trajectory results from a different initial phase point in the ground state (same initial energy) but excited and allowed to cross back to the ground state in precisely the same manner as the trajectory of Figure 4. For the first picosecond or so the trajectories of Figures 4 and 5 are similar. Then instead of recombining, the Br atoms remain well separated—on the X state but sufficiently far out that they feel very small attractive forces. An argon atom has clearly come between the two Br atoms which then remain at the surface of the cluster. Note that f_{bond} is oscillating with a longer and more variable period typical of the solvent motion rather than the Br_2 vibration. Note also that there

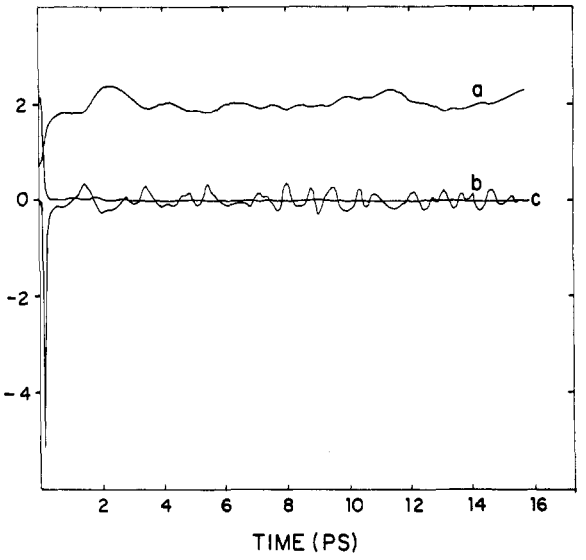

Figure 5. Excitation and "solvation" dynamics of 10 K Br_2Ar_{20} cluster excited to $^1\Pi_{1u}$ state: (a) Br_2 bond distance; (b) f_{bond}; (c) Br_2 bond energy. For units see caption of Figure 4.

is no relaxation in energy below the gas-phase dissociation threshold since the Br_2 is trapped in the wing of its potential ($V = 0$).

These two behaviors are typical in the sense that they are well represented in the population of trajectories performed. About 30% (26 out of 80) Br_2Ar_{20} trajectories followed for 5 ps did not show recombination. We have also generated longer trajectories. For some of these recombination was not observed after more than 10 ps. The dissociation trajectory is really analogous to the secondary cage effect in liquids, in which the radicals escape and become separately solvated. We can surmise that the tendency to recombine will be stronger in clusters than in liquids (other factors being equal), since there is no isotropic liquid outside the first shell balancing the central attractive forces in the cluster. At this excitation energy there was never a loss of a bromine atom from the cluster. Of course the Br atoms should eventually recombine.

Similar trajectories excited to $1.5D_e$ on the X state show only the immediate recombination behavior. This is to be expected from the hard-sphere collision model. Even though bromine excited in this fashion has more kinetic energy at the time of collision than for excitation to the $^1\Pi_{1u}$ state, it loses about 8/9 of that kinetic energy and falls below the dissociation threshold. The solvation behavior has not been observed for this case. Trajectories generated following Franck–Condon excitation to the B state also showed the immediate recombination behavior. Here again the contact between the bromine atoms and the cage occurred when Br_2 was in an attractive region of the B-state potential. We have not made a detailed study of the dynamics of this last system which involves $B \rightarrow {}^1\Pi_{1u} \rightarrow X$ surface hopping.

B. Br_2Ar_{70} Recombination Dynamics. We have not yet run multiple long-time trajectories on the large cluster because of the amount of computer time required; thus, we have not ascertained a 5-ps recombination probability for this cluster. One strong indication that it will be much higher in the larger system is that the maximum r_{Br-Br} value achieved is only 1.6σ for Br_2Ar_{70} while it may reach 1.9σ or 2.0σ in the smaller cluster. This means that two bromine atoms do not really get far enough apart to permit an argon atom to come between them. More important differences between the single- and double-shell systems appear when we consider the relaxation behavior of those bromines that do recombine. This will be the subject of the next section.

V. Relaxation Dynamics

Let us now focus on the Br_2 molecule and its effect on the van der Waals cluster after the diatomic recombines and is left vibrationally hot in the X state. The Br_2 vibrationally relaxes by

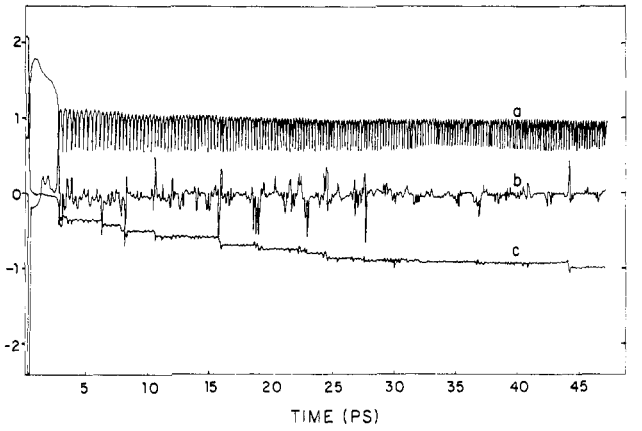

Figure 6. Excitation dynamics and recombination dynamics of 10 K Br_2Ar_{20} cluster, long-time behavior: (a) Br_2 bond distance; (b) f_{bond}; (c) Br_2 bond energy. For units, see Figure 4. Note that snapshots in Figure 7 are taken from this trajectory.

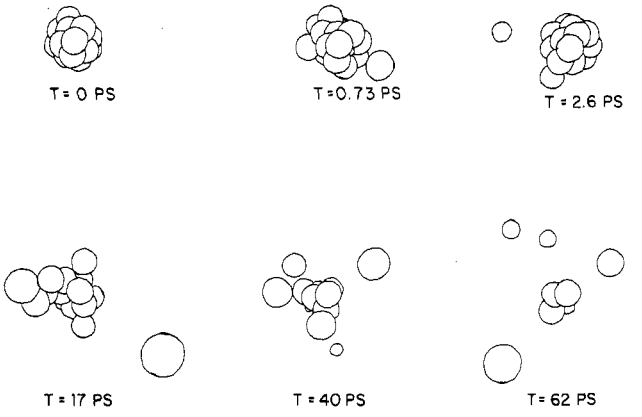

Figure 7. Instantaneous configurations (snapshots) of Br_2Ar_{20} cluster. Same trajectory as in Figure 6. Cluster is viewed such that Br_2 bond orientation is always as in Figure 2a (Br_2Ar_8 cluster). Oversize circles represent argon atoms which are leaving the cluster in the direction of the viewer, while undersized circles represent atoms moving in the opposite direction.

giving up its energy to the van der Waals modes of the cluster. Some natural questions to ask are the following: How does the rate of this relaxation compare to the corresponding rate for a bulk liquid system? How is energy dissipated in the cluster in contrast to the bulk system? To begin to answer these questions we have generated long trajectories for the Br_2Ar_{20} and Br_2Ar_{70} clusters (one and two solvent shells, respectively).

A. Br_2Ar_{20} Relaxation. The two questions that we have just asked are of course intimately related. Figure 6 shows the time dependence of a number of bromine properties, as in Figure 4. After recombination, the bromine molecule is left at an energy of about -20 to -16 ϵ. It then relaxes slowly; the energy record shows relatively flat plateaus punctuated by sudden losses in energy of 2–3 ϵ corresponding to one or more vibrational quanta. These losses in energy are highly correlated with positive and negative spikes in the record of f_{bond}. This strongly suggests that the bromine loses energy by an impulsive mechanism. In fact one can ascertain from the record of configurations of the cluster that the negative spikes correspond to collisions between a bromine atom and an argon in a cap position on that side of the cluster. The positive spikes correspond to a collision in which the bromine atoms strike an argon atom which moves partially into the space between them; the diatomic is effectively squeezing the argon at the inner turning point. The relatively long time between large force spikes (or relatively long flat energy record segments) is due to the fact that the 20-atom cluster is rapidly heated and has a loose, expanded nonrigid or liquid structure.

The slow rate of energy decay appears to confirm the "stagnation" effect discussed by Wilson and co-workers.[5] Before

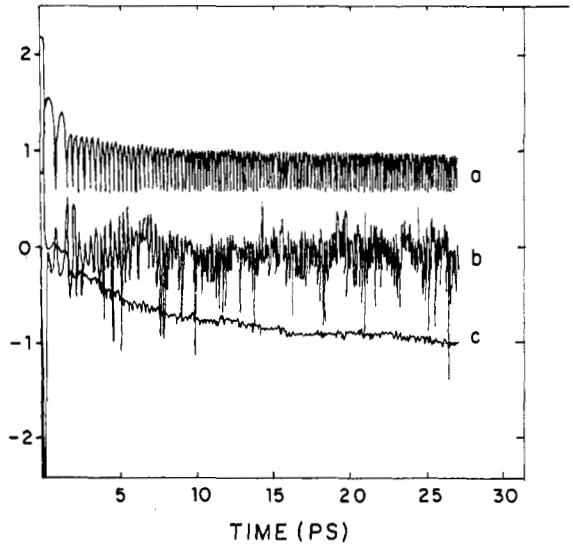

Figure 8. Excitation and recombination dynamics of 10 K Br_2Ar_{70} cluster excited to the $^1\Pi_{1u}$ state: (a) Br_2 bond distance, (b) f_{bond}, (c) Br_2 bond energy. Units as in Figure 4.

too much significance is attached to this stagnation, we should note the effect that the energy transfer has on the rest of the cluster. Figure 7 shows a series of snapshots of the cluster at various times between 0 and 60 ps. It is immediately obvious not only that the cluster is loose and nonrigid but that argon atoms are leaving the cluster fairly regularly. In fact after 60 ps, 15 of the original 20 argon atoms have left the cluster. It is noteworthy that the Br_2 molecule is left in a highly excited vibrational state even after losing its whole solvation sphere. While vibrational stagnation is inevitable for an isolated molecule, the Br_2Ar_{20} simulation *does* indicate that the argons evaporate from the cluster as a result of direct impulsive collisions with the bromine atoms; the alternative mechanism in which evaporation is viewed as a unimolecular decay from an activated (hot) cluster appears to be ruled out for the Br_2Ar_{20} system.

A surprising confirmation of the validity of the impulsive model is found in the work of Valentini and Cross;[24] in this experiment an iodine molecule within an I_2Ar complex was excited to about 434 cm^{-1} above the dissociation limit of the B state. No I radicals were observed but transitions from bound vibrational levels were seen in the dispersed fluorescence spectrum. This is evidence for a single atom cage effect which could only occur if the complex is linear. A very rough calculation of the final bound-state vibrational quantum number has been made.[25] by using an approximate I_2–Ar van der Waals potential. The calculation clearly shows that the impulsive model predicts the large range of final states (v = 23 to v = 49, experimentally).

B. Br_2Ar_{70} Relaxation. The energy vs. time record for bromine relaxation in a 70-atom cluster is given in Figure 8. The energy loss is smoother and more rapid in the Br_2Ar_{70} case. After the initial caging collision two argon atoms are lost. No argon atoms are lost from the cluster during the next 26 ps. It appears that the second shell of atoms serves to keep the whole structure much more rigid, confining the bromine and enabling a more efficient transfer of energy. A series of snapshots (Figure 9) from the Br_2Ar_{70} trajectory shows how little the structure of the cluster is disturbed by the energy transfer in comparison to the Br_2Ar_{20} case. There is clearly an increase in the fluidity of the system, but there is no dramatic breakup of the cluster. It is more likely that the unimolecular decay mechanism is at work in the evaporation of argon atoms from the large system. Energy must be transferred from the first coordination shell to the second shell before a surface atom can be kicked off. It is not possible to

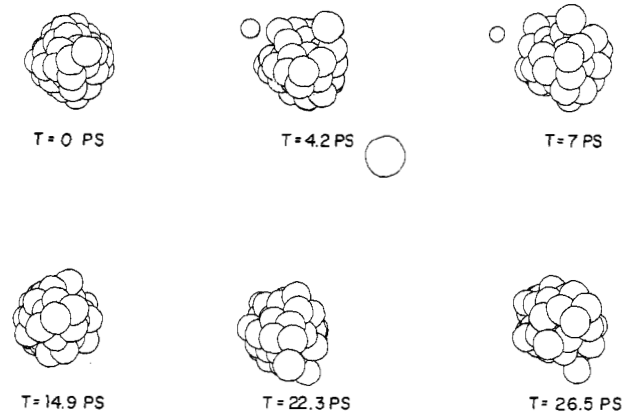

Figure 9. Snapshots of Br_2Ar_{70} cluster of Figure 8. See caption of Figure 7.

confirm this at the present time because of the extremely long trajectories that have to be generated.

VI. Conclusion

It is interesting to note that the stagnation effect in the X state noticed by several authors[5,7] may be accentuated in clusters by a nonlinear resonance mechanism.[26] This phenomenon is manifested as a sudden increase (or decrease) in the rate of energy transfer, because anharmonicity of donor and acceptor modes causes their mechanical frequencies to come into (go out of) resonance. For the anharmonic donor vibrational model (Br_2), the mechanical frequency increases with decreasing energy. Only when the Br_2 is near the dissociation limit is there a frequency match and efficient V–T energy transfer to the cluster cage. The mismatch in frequency of the Br_2 vibration and the argon van der Waals modes is accentuated as the Br_2 loses energy to the argon, because the anharmonic cluster bonds show a decrease in mechanical frequency with increasing energy. This behavior leads to a more marked stagnation effect in clusters than in the bulk liquid, since in the latter case a local hot spot may be cooled by dissipative processes whereas, in small clusters, evaporation is the only means of cooling the bromine's environment. Indeed, the breakup of the Br_2Ar_{20} cluster may be regarded as an extreme example of the nonlinear resonance phenomenon, resulting in energy trapping in a local mode! The van der Waals modes go to zero frequency as the atoms evaporate, leaving the Br_2 without a cluster to which it can surrender its residual energy.

We have observed, as did Nesbitt and Hynes,[7] that fast component of Br_2 vibrational relaxation near the dissociation limit. They attribute this component to V–T transfer between soft spheres, while we have explained it qualitatively by a simple hard-sphere collision model. The rate of energy transfer in our system is smaller than that of I_2/CCl_4 studied by Nesbitt and Hynes,[7] since there is no analogue to the V–V transfer in our rare gas cluster. The stagnation is more pronounced than in the I_2/Xe simulation of Wilson and co-workers[5] because of the evaporation effect discussed above. We do not as yet have any explanation for the results of Kelley and Rentzepis[4] except that unlike the site–site potential used here the real Br_2–argon potential may depend strongly on Br_2 bond length—an effect that may be manifested in an r dependence of ϵ and σ.

We have investigated the effect of variable cluster size on the relaxation rate of Br_2 photoexcited to the repulsive $^1\Pi_{1u}$ state. Initial cluster conditions correspond to a microcrystallite. Recombination is more likely for the larger cluster, and vibrational relaxation of the Br_2 in the X state is faster for larger clusters. Graphs of f_{bond} (defined in eq 6) vs. time have proved most useful in following the details of the classical dynamics of the collision(s) of Br_2 with its solvent cage. In particular Figure 6 shows that both outer turning point and inner turning point collisions can

(24) Valentini, J. J.; Cross, J. B. *J. Chem. Phys.* **1982**, *77*, 572.
(25) Amar, F., unpublished work.
(26) Sibert, E. L., III; Reinhardt, W. P.; Hynes, J. T. *Chem. Phys. Lett.* **1982**, *42*, 455.

be effective in transferring energy from the Br_2 to the cage.

It will be interesting to investigate the temperature dependence of the recombination and relaxation processes. How do these processes change as the cluster initial conditions are altered from microcrystallite to microdroplet? We can surmise that recombination will be slower for hotter clusters.

Acknowledgment. This work was supported by grants from the National Science Foundation.

Registry No. Br_2, 7726-95-6.

Glass-Forming Microemulsions: Vitrification of Simple Liquids and Electron Microscope Probing of Droplet-Packing Modes

J. Dubochet, M. Adrian,

European Molecular Biology Laboratory, Heidelberg, West Germany

J. Teixeira,

Laboratoire Leon Brillouin,† CEN-Saclay-91191 Gif-sur-Yvette Cedex, France

C. M. Alba,§ R. K. Kadiyala,‡ D. R. MacFarlane,⊥ and C. A. Angell*

Department of Chemistry, Purdue University, West Lafayette, Indiana 47907 *(Received: September 27, 1984)*

The recent development of microemulsion systems which do not separate during cooling and in which neither dispersed nor matrix phases crystallize during the cooling process permits low-temperature studies of the microemulsion structure and the investigations of common liquids in unusual states. Benzene, carbon tetrachloride, and CS_2 all can be supercooled without limit in microemulsion form, and their glass transition temperatures have been determined. Transmission electron microscopy of thin vitrified layers permits high-resolution observations of water-diluted samples of the same microemulsions. Gas-like, liquid-like and solid-like (hexagonal) organization of the microemulsion droplets are observed. Other experiments must decide which of these structures are imposed by the thin-film preparation technique and which are natural arrangements of warm bulk microemulsions.

Introduction

Recently, pseudoternary oil-in-water microemulsions which remain stable during continuous rapid cooling and which finally vitrify at $T < 165$ K were described.[1] In these microemulsions, the matrix phase is a propylene glycol aqueous solution which itself vitrifies at 165 K. The oil phase in the initial study was *o*-xylene but can be a wide variety of other molecular liquids as we show below. In the case reported, the *o*-xylene was shown to retain the same fluidity characteristics as the xylene in ordinary emulsions which in turn was virtually unchanged from that in the bulk, implying that the surface forces in the microemulsion effectively compensate for the small size effect of the microscopically dispersed phase. Indeed, this would be expected from the fact that microemulsions can coexist with excess the almost-pure "oil" phase, implying that the chemical potential of the oil in the droplet phase is not depressed much.

The existence of these systems offers unusual opportunities to study not only the properties and structure of microemulsions in the absence of rapid exchange across the microdroplet surfaces—a characteristic of microemulsions observed at ambient temperature—but also the properties of liquids which depend on avoiding certain long-range fluctuations, e.g. those which lead to crystallization.

Another approach to the study of microemulsions is offered by the recently developed thin-film vitrification method[2] in which ultrafast cooling allows the vitrification of many liquids, including pure water, in a form suitable for electron microscopy.

In the present paper we will report on exploitations of these two possibilities. Firstly, we will examine the possibility of vitrifying liquids usually thought of as "simple" or "normal" and thereby helping to establish the view that the glass transition is in principle a universal characteristic of the liquid state.[3] Secondly, we use cryoelectron microscopy for the study of possible droplet-packing modes in a less viscous variant of the basic microemulsion.

Experimental Section

To explore the variety of simple liquids which can be obtained in microemulsion form and vitrified, it was assumed that the same principles underlying microemulsification of xylenes observed in the earlier study would apply to the additional liquids investigated here. Therefore, we simply titrated an initial mixture of one part of molecular liquid and two parts of aqueous phase (propylene glycol + water in mole ratio 1:3) with a solution of one part of molecular liquid and two parts of surfactant (by volume). This procedure, which amounts to moving along the line AB in the pseudo-three-component phase diagram (reproduced from an earlier publication[1] in Figure 1), maintains the volume fraction of molecular liquid constant at 33 vol % during the titration procedure. The sample container was shaken after each addition until a clear phase suddenly appeared. The composition at which this occurred was always close to that observed in the finger region in Figure 1, though in the cases of benzene and CCl_4 no sign of

† Laboratoire mixte CEA-CNRS.

‡ Present address: Medical School, Stanford University, Stanford, CA 94305.

§ Permanent address: Laboratoire de Chimie Physique, 11, rue Pierre et Marie Curie, 75231 Paris, France.

⊥ Present Address: Department of Chemistry, Monash University, Clayton, Victoria 3168, Australia.

(1) (a) Angell, C. A.; Kadiyala, R. K.; MacFarlane, D. R. *J. Phys. Chem.* **1984**, *88*, 4593. (b) First reported in: MacFarlane, D. R.; Angell, C. A. *J. Phys. Chem.* **1982**, *86*, 1927.

(2) (a) Dubochet, J.; McDowell, A. W. *J. Microsc. (Oxford)* **1981**, *124*, RP3-RP4. (b) Dubochet, J.; Lepault, J.; Freeman, R.; Berryman, J. A.; Homo, J. U. *J. Microsc. (Oxford)* **1982**, *128*, 219. (c) Dubochet, J.; Adrian, M.; Vogel, R. H. *Cryo-Lett.* **1983**, *4*, 233. (d) Adrian, M. Dubochet, J.; Lepault, J.; McDowall, A. W. *Nature (London)* **1984**, *308*, 42.

(3) Cohen, M. H.; Turbull, D. *J. Chem. Phys.* **1960**, *34*, 120.

0022-3654/84/2088-6727$01.50/0